NMR Study of General Anesthetic Interaction with nAChR β_2 Subunit

Vasyl Bondarenko,* Victor E. Yushmanov,* Yan Xu,*† and Pei Tang*†‡
Departments of *Anesthesiology, †Pharmacology, and ‡Computational Biology, University of Pittsburgh School of Medicine, Pittsburgh, Pennsylvania

ABSTRACT The molecular basis of anesthetic interaction with membrane proteins has been explored via determination of anesthetic effects on the structure and dynamics of the extended second transmembrane domain (TM2e) of the human neuronal nicotinic acetylcholine receptor (nAChR) β_2 subunit in dodecylphosphocholine (DPC) micelles by ^{1}H and ^{15}N solution-state NMR. Both 1-chloro-1,2,2-trifluorocyclobutane (F3) and isoflurane, two volatile general anesthetics, induced nonuniform changes in chemical shifts among residues in TM2e. Saturation transfer difference NMR experiments further confirmed the direct anesthetic interaction with TM2e. A significant and more specific anesthetic interaction was observed on three leucine residues at the helix C-terminus. Although the TM2e helical structure remained after addition of anesthetics, plausible shortening and lengthening of helix hydrogen bonds were evidenced by periodic changes in backbone amide chemical shifts. The TM2e backbone dynamics were determined on the basis of the ^{15}N relaxation rate constants, R_1 and R_2, and the ^{15}N-[^{1}H] NOE using the model-free approach. The global tumbling time (11.7 ns) of TM2e in micelles slightly increased (~12.3–12.5 ns) in the presence of anesthetics. The order parameter, S^2, exceeded 0.9 for all ^{15}N-labeled residues, showing a restricted internal motion. Anesthetics appear to have minor effect on the TM2e's internal motion. This study provided the basis for subsequent more comprehensive studies of anesthetic effects on the transmembrane domain complex of neuronal nAChR.

INTRODUCTION

The molecular mechanism of general anesthesia remains an enigma. After more than a century of clinical practice, no one knows with certainty how high-order functions of the central nervous system can be disrupted reversibly by general anesthetic molecules. The obstacle for a comprehensive understanding lies in the complexity of the central nervous system and the lack of powerful tools that allow us to straightforwardly find answers to this unsolved mystery.

Nicotinic acetylcholine receptors (nAChRs) (1,2), along with other members in the superfamily of cys-loop receptors (3), have been identified as potential targets of general anesthetics (4,5). They are pentameric channel proteins responsible for the fast synaptic transmission in the central and peripheral nervous systems. Each of five subunits of a receptor comprises an extracellular domain, four transmembrane domains, an intracellular domain, and loops that link these domains. The second transmembrane domain (TM2) of each subunit lines the pore of a channel. Site-directed mutagenesis within the TM2 domain showed markedly changed sensitivity of nAChR to anesthetics, indicating possible anesthetic-sensitive sites in the TM2 (6–8). The ^{19}F nuclear magnetic resonance study of anesthetic isoflurane binding to nAChR reconstituted in phospholipid bilayers suggested no more than two specific binding sites in each subunit of nAChR and a nonspecific interaction with the lipid phase (9). Anesthetic halothane direct photoaffinity labeling of the *Torpedo* nAChR in native membranes demonstrated multiple similar binding domains for halothane in the transmembrane region of the nAChR (10). Halothane photolabeling of residue Tyr-228 in the δ-subunit of *Torpedo* nAChR was later identified (11). More recently, a photoactivatable analog of the intravenous general anesthetic etomidate was found to label several residues in α- and δ-subunits of *Torpedo* nAChR in a state-dependent and subunit-selective fashion (12). These studies provided valuable information for potential anesthetic binding sites in nAChR. However, further investigation is necessary to prove whether findings on *Torpedo* nAChR can be generalized for other types of nAChR, considering that many potential anesthetic binding sites suggested by photolabeling were highly subunit dependent. Moreover, to gain insights into how anesthetics alter the protein functions, we need to know not only anesthetic binding sites but also the structural and dynamic consequences of nAChR in response to the anesthetic interaction.

The structure determination of an intact receptor protein, such as nAChR, has proven extremely difficult. The currently available structure model for *Torpedo* nAChR, obtained using cryo-EM with 4 Å resolution (13,14), is invaluable to serve as a structure template for other members in the cys-loop receptor family, although there are still unsolved segments and loops in the structure. The high-resolution structures of intact neuronal nAChRs that are more sensitive than *Torpedo* nAChR to volatile general anesthetics have not been experimentally determined yet, and these determinations are unlikely to be resolved any time soon because of the tremendous technique challenges. A more realistic approach

Submitted July 4, 2007, and accepted for publication October 3, 2007.

Address reprint requests to Professor Pei Tang, PhD, 2049 Biomedical Science Tower 3, 3501 Fifth Avenue, University of Pittsburgh, Pittsburgh, PA 15260. Tel.: 412-383-9798; Fax: 412-648-8998; E-mail: tangp@anes.upmc.edu.

Victor E. Yushmanov's present address is Department of Anesthesiology, Allegheny-Singer Research Institute, Pittsburgh, PA 15212.

Editor: Mark Girvin.

0006-3495/08/03/1681/08 $2.00

doi: 10.1529/biophysj.107.116772

is a systematic reduction-rebuild approach. An excellent demonstration of this approach is the study of the 3-D structure of the G-protein-coupled receptor rhodopsin (15). Using the same approach, we obtained high-resolution structures of transmembrane domains of neuronal nAChR β_2 subunit on the basis of NMR experiments (16,17), which provided the structural basis for characterizing anesthetic interaction with neuronal nAChRs. It is worth mentioning that neuronal nAChRs containing β_2 subunits are particularly sensitive to volatile general anesthetics (7,18,19).

In our study, we determined effects of two volatile general anesthetics, isoflurane and 1-chloro-1,2,2-trifluorocyclobutane (F3), on the structure and backbone dynamics of a peptide segment corresponding to the extended TM2 domain of the human neuronal nAChR β_2 subunit (TM2e). The atomistic resolution of NMR spectra allows us to identify residues interacting with anesthetics and to determine the structure and dynamics consequences of the TM2e on the anesthetic interaction. The knowledge gained from this study laid the ground for further investigation of general anesthetic effects on multidomain complex targets.

MATERIALS AND METHODS

Sample preparation

The extended TM2 domain (TM2e) of the human neuronal nAChR β_2 subunit, including residues EKMTLCISVLLALTVFLLLISKIVPPTS (molecular mass of 3.05 kDa), was obtained by solid-phase synthesis as described previously elsewhere (16,17). All seven leucine residues were selectively ^{15}N labeled. For reconstitution of the TM2e peptide into DPC micelles, TM2e dissolved in trifluoroethanol (Sigma, St. Louis, MO) was added to an aqueous solution of DPC (Avanti Polar Lipids, Alabaster, AL) to reach desired surfactant/peptide molar ratios. Typically, there are 1–3 mM TM2e and 100–450 mM DPC in the sample. The samples were lyophilized after vigorous mixing and rehydrated with 10% D_2O for deuterium lock in NMR measurements. Two samples of 50 mM DPC in 90% H_2O and 10% D_2O were prepared as control for ^{1}H saturation transfer difference (STD) experiments. DPC-d_{38} and D_2O were obtained from Cambridge Isotope Laboratories (Andover, MA). Volatile anesthetics isoflurane (Abbott Laboratories, North Chicago, IL) and F3 (PCR, Gainesville, FL), shown in Fig. 1, were added directly to the NMR samples using a gas-tight microsyringe.

NMR spectroscopy

The majority of NMR spectra were recorded at 30°C on a Bruker Avance-600 NMR spectrometer (^{1}H: 600.03 MHz; ^{15}N: 60.81 MHz) equipped with a triple-resonance inverse-detection cryoprobe, TCI (Bruker Instruments, Billerica, MA). The TM2e chemicals shift assignment was accomplished previously (16) using ^{1}H TOCSY and NOESY experiments as well as ^{15}N-filtered NOESY experiments. Fluorinated anesthetics added to the samples were quantified by ^{19}F NMR on a Chemagnetics CMX-400SLI spectrometer (^{19}F: 377.37 MHz; Otsuka Electronics, Fort Collins, CO) using aqueous solutions of trifluoroacetic acid as external references for the chemical shift and concentration. ^{15}N-decoupled ^{1}H homonuclear two-dimensional nuclear Overhauser effect (NOE) spectroscopy (NOESY) data were typically acquired at 600.03 MHz into 2048 t_2 and 640 t_1 data points with a spectral width of 10 ppm in each dimension, 72 to 80 transients per increment, and 100-ms mixing time. The WATERGATE pulse scheme (20) was applied for water suppression. The States-TPPI method was used for quadrature detection in the indirect dimension (21). Gradient-selected sensitivity-enhanced ^{1}H-^{15}N heteronuclear single quantum correlation (HSQC) data were typically acquired into 2048 t_2 and 80 t_1 data points, with spectral width of 12–14 ppm for ^{1}H and 15 ppm for ^{15}N. To confirm anesthetic interaction with TM2e, ^{1}H STD experiments (22) were performed on samples containing 10 mM isoflurane or 13 mM F3 in the presence and absence of TM2e on a Bruker Avance-800 MHz spectrometer. Water suppression was achieved using excitation sculpting with gradients (23). TM2e signals were not filtered. A STD spectrum was obtained by subtracting a pair of spectra ($\Delta I = I_{off} - I_{on}$) acquired in an interleaved fashion with on- and off-resonance frequencies of 0.6 ppm and 15 ppm, respectively. A series of STD spectra were collected with a low saturation power of 20 Hz at different saturation times, including 1, 2, 4, 7, and 10 s. Each STD spectrum was a sum of 256 scans. The recycle delay of 20 s was found adequate for ^{1}H relaxation and used in the experiment. Spin-lattice (R_1) and spin-spin (R_2) ^{15}N relaxation rate constants, and ^{15}N-[^{1}H] NOE values were repeatedly measured at 600.03 MHz for each of the ^{15}N amides using standard pulse sequences (24) with echo-antiecho gradient selection (25,26). Typically, 80 t_1 data points were used with recycle delays of 2.3 s or 1.8 s for R_1 and R_2 measurements, respectively. There were nine variable delays ranging from 20 to 1800 ms for R_1, and 17 to 170 ms for R_2. In NOE experiments, 80 indirect data points were acquired with or without proton saturation in interleaved fashion. Saturation was achieved by a train of 120° pulses at 5-ms intervals for duration of 3 s. ^{1}H chemical shifts were referenced to the 2,2-dimethyl-2-silapentane-5-sulfonate (DSS) resonance at 0 ppm, and ^{15}N chemical shifts were referenced indirectly (27).

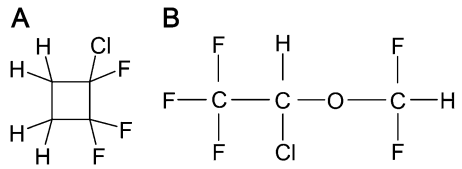

FIGURE 1 Chemical structures of the volatile anesthetics (*A*) F3 and (*B*) isoflurane.

Data processing and analysis

All NMR spectra were processed using NMRPipe and NMRDraw (28) with a linear prediction or zero filled to double or quadruple data points in each spectral dimension and analyzed using Sparky (29). The NOE on anesthetics from TM2e was calculated by $(I_{off} - I_{on})/I_{off}$, where I_{off} and I_{on} are the anesthetic peak intensities in STD spectra acquired off and on resonance of TM2e, respectively. NOE errors were derived from spectral signal/noise ratios (24). The ^{1}H and ^{15}N chemical shift changes of TM2e induced by anesthetics were obtained by subtracting individual peak frequencies in a pair of NMR spectra acquired without and with anesthetics. Typically each processed HSQC spectrum had 4096 × 512 data points, giving an uncertainty of 0.004 or 0.03 ppm for the ^{1}H and ^{15}N frequency readings. ^{15}N R_1 and R_2 values were determined from two-parameter fits of peak intensities versus variable delay to single exponential functions. ^{15}N-[^{1}H] NOE values were reported as peak intensity ratios obtained with and without ^{1}H saturation. The global tumbling time (τ_m) was initially estimated from the R_2/R_1 ratio (30) and refined by fitting experimentally measured R_1, R_2, and NOE values in the framework of Lipari-Szabo formalism (31,32) and subsequent Monte Carlo numerical simulations using the Modelfree software package (33,34) or using the Tensor-2.0 program (35). All the models in the ''Modelfree'' package were tested for model selection. Our R_1, R_2, and NOE data were best described using the model that included the squared order parameter (S^2) but excluded the exchange rate constant and the effective correlation time for fast internal motions. Therefore, this model was chosen for final relaxation data analysis.

RESULTS

Direct interaction of isoflurane or F3 with TM2e was confirmed by the STD experiments. Fig. 2 *A* displayed representative STD spectra at selected saturation times for TM2e with 10 mM isoflurane and 13 mM F3. Peak intensities (ΔI) of isoflurane and F3 in the STD spectra resulted from a pair of spectra, acquired in an interleaved fashion, with the saturation frequency off and on resonance of TM2e ($\Delta I = \Delta I_{off} - \Delta I_{on}$). If anesthetics had no direct contact with proteins, their nuclear magnetization would not be affected by saturating protein magnetization, and then anesthetic signals would be canceled in a STD spectrum ($\Delta I = 0$). If anesthetics interacted with proteins, longer saturation time would lead to more magnetization transfer until it reached a steady state. Apparently, both isoflurane and F3 had close contact with TM2e. Fig. 2 *B* illustrated the relative amount ($\Delta I/\Delta I_{off}$) of magnetization transferred to isoflurane or F3 from TM2e at different saturation times. The same STD experiments were repeated under the same sample conditions but without TM2e (see Fig. 1S in Supplementary Materials). No anesthetic signals were detected in STD spectra (Fig. 1S, *A′* and *B′*), confirming that the observed isoflurane and F3 signals in the presence of TM2e indeed result predominately from direct anesthetic interactions with TM2e.

The presence of F3 or isoflurane perturbed the ^{1}H and ^{15}N chemical shifts of TM2e in DPC micelles. As revealed from ^{1}H-^{15}N-HSQC spectra in Fig. 3, both anesthetics induced upfield (such as L5) and low-field (L19) shifts. The peak displacement was inhomogeneous along the TM2e sequence. Of all the leucine amides, L5 is most sensitive to both anesthetics. The differences in the patterns of HSQC chemical shift changes on addition of F3 and isoflurane are minor, but isoflurane has noticeably greater effects on L11 than F3. L19 is more sensitive to F3 than to isoflurane. The dependencies of the leucine peak displacements on the anesthetic concentrations are demonstrated in Fig. 4. The overall magnitude of anesthetic effect is presented using the weighted average of the ^{15}N and ^{1}H chemical shifts of selected amide groups, defined as $\Delta\delta_{HN} = [(\Delta\delta_H^2 + \Delta\delta_N^2/25)/2]^{1/2}$ (36). The changes in chemical shifts increase linearly with the elevation of anesthetic concentrations in a certain range. It is worth mentioning that chemical shifts of all leucine residues, except L5, became insensitive to additional amounts of anesthetics when anesthetic concentration went beyond a few millimolar in range (Fig. 2S).

Anesthetic effects on the TM2e structure were determined by measuring the anesthetic-induced $^1H_\alpha$ and ^1H_N shifts for all residues of TM2e through ^{1}H NOESY NMR spectra. As demonstrated in Fig. 5 *A*, variations of H_α chemical shifts

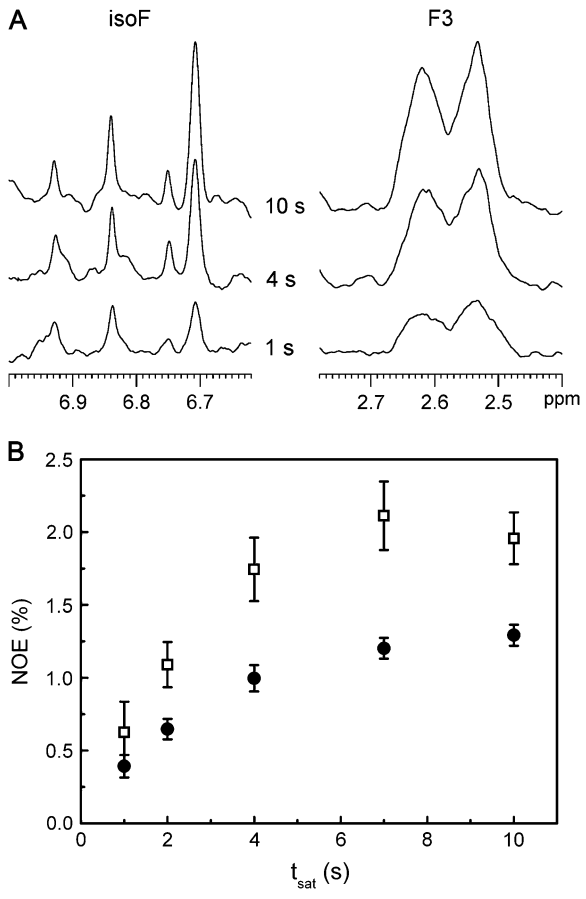

FIGURE 2 (*A*) Saturation transfer difference (STD) spectra of 1 mM TM2e in 50 mM of DPC micelles at marked saturation times in the presence of 10 mM isoflurane (*left*) and 13 mM F3 (*right*). (*B*) NOE on isoflurane (□) and F3 (●) as a function of the saturation time. NOE was measured by $(I_{off} - I_{on})/I_{off}$, and NOE uncertainties were determined by the signal intensity and noise level. Notice the NOE steady-state regime at longer saturation times.

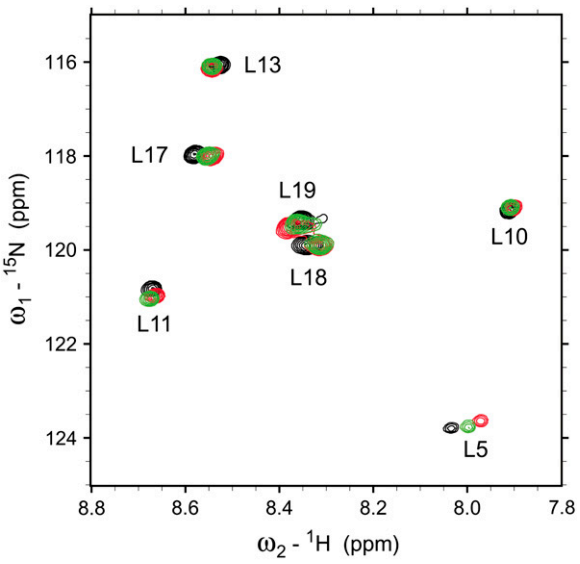

FIGURE 3 Overlay of ^{1}H-^{15}N HSQC NMR spectra of 1.0 mM TM2e (^{15}N-labeled leucine) in 150 mM DPC in the absence (*black*) and presence of 14 mM F3 (*red*) or 11 mM isoflurane (*green*).

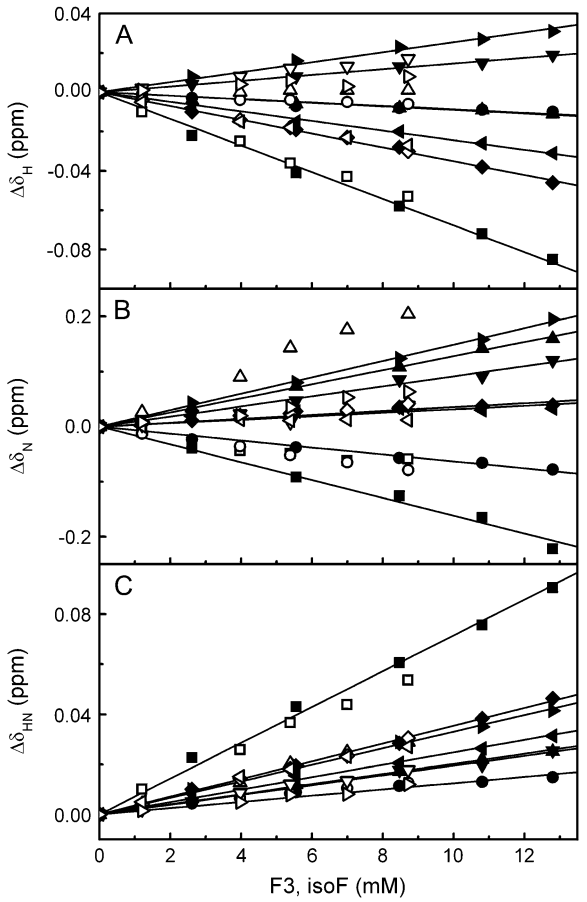

FIGURE 4 Changes in (*A*) ^{1}H and (*B*) ^{15}N chemical shifts of amide NH of 2 mM TM2e in 100 mM of DPC micelles are modulated by anesthetic F3 (*solid symbols*) and isoflurane (*open symbols*). (C) The complex change in chemical shifts, $\Delta\delta_{HN}$, was calculated using $\Delta\delta_{HN} = ((\Delta\delta_H^2 + (\Delta\delta_N^2/25))/2)^{1/2}$. The symbols for each Leu are: ■, L5; ●, L10; ▲, L11; ▼, L13; ♦, L17; ►, L18; ◄, L19. Data were obtained from ^{15}N-HSQC NMR spectra in the absence and presence of various concentrations of F3 or isoflurane. The solid lines resulted from the least-squares fitting of the changes in leucine chemical shift induced by varying F3 concentrations.

induced by the addition of anesthetics were generally small. The secondary chemical shift index based on deviations of H_α proton chemical shifts from their random coil values (37) in the absence and presence of anesthetics showed the value of -1 for most of the TM2e residues, suggesting that anesthetics did not significantly modify the TM2e secondary structure (16). The secondary shifts of the amide protons (H_N) are more sensitive to anesthetics than H_α. Fig. 5 *B* showed that F3 induced changes in the H_N chemical shift along the TM2e sequence, where the positive and negative change represented H_N down- and up-field shift relative to the resonances without anesthetics, respectively. The periodicity of H_N chemical shifts along a protein sequence could be observed from helical proteins and was interpreted mainly resulting from a shortening of hydrogen bonds (HBs) on the hydrophobic side of helices and a lengthening of HBs on the hydrophilic side (38). A weak periodicity in the change of

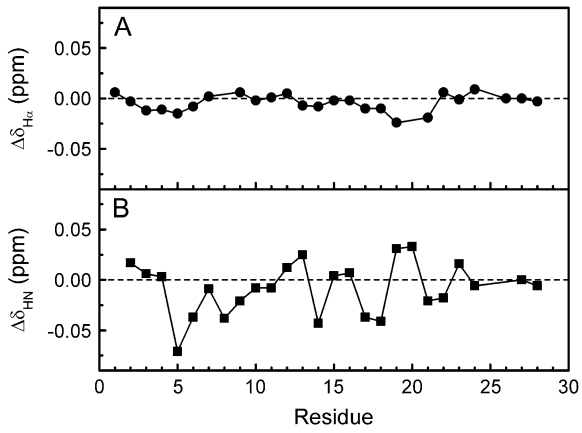

FIGURE 5 Anesthetic F3 induced changes in (*A*) $^1H_\alpha$ and (*B*) ^1H_N chemical shifts of 1.0 mM TM2e in 150 mM of DPC-d_{38} micelles. Data were obtained from NOESY spectra in the absence and presence of ~20 mM F3.

the H_N chemical shift occurred after the addition of anesthetics (Fig. 5 *B*). Although it is impossible to quantify HB changes solely based on the H_N chemical shift changes, such a periodic change suggested the possibility of subtle shortening or lengthening of HBs on different sides of TM2e and a certain degree of helical curvature induced by anesthetics, as depicted in Fig. 6.

The anesthetic effects on the backbone dynamics of TM2e were determined by ^{15}N relaxation of seven selectively ^{15}N-

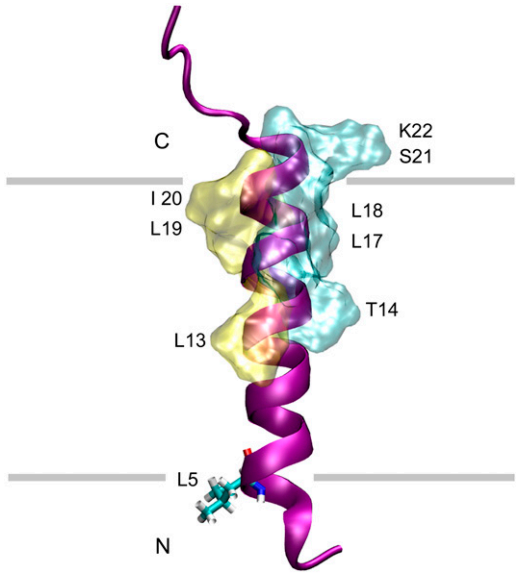

FIGURE 6 Molecular surface representation of the TM2e structure in DPC micelles delineating a sensitivity of different residues along the TM2e chain to anesthetic F3 using the magnitude and direction of F3-induced amide proton shifts (Fig. 4 *B*) as criteria. The residues having lengthened or shortened HBs are labeled and covered with cyan and yellow surface, respectively. Leu 5 is also colored in cyan. The gray lines highlight putative membrane surfaces. The TM2e structure in DPC was calculated as described elsewhere (16).

labeled leucine residues. As summarized in Fig. 7, addition of either anesthetic (F3 or isoflurane) resulted in a downward trend in R_1 and an upward trend in R_2 for most of leucines. The trend became even more apparent when the amount of anesthetic reached more than 10 molcules per DPC micelle (see Fig. 3S). The opposite trends of R_1 and R_2 change indicate a slower global tumbling of the micelle-bound TM2e. Indeed, the R_2/R_1 ratio for those residues whose relaxation is not affected by the fast internal motions on the picosecond time scale is virtually independent of the internal motion and provides an initial estimation for the reorientation time of each NH vector with global tumbling, i.e., the τ_m of the peptide (30). The τ_m of TM2e in DPC, obtained from the R_2/R_1 ratio and averaged over all leucine residues except L5, yielded 11.7 ns in the absence of anesthetics and 12.5 and 12.3 ns in the presence of 13 mM F3 or 9 mM isoflurane, respectively. The NOE values were elevated slightly in residues L5 and L19 but slightly lower or unchanged in other leucine residues after addition of anesthetics. The square order parameter S^2, as shown in Fig. 7 *D*, was derived later by further analysis of the NMR relaxation data using a model-free approach (31,32). The values of S^2 are greater than 0.9 for all leucine residues, with or without anesthetics, indicating that all leucines are located in regions with restricted internal motions.

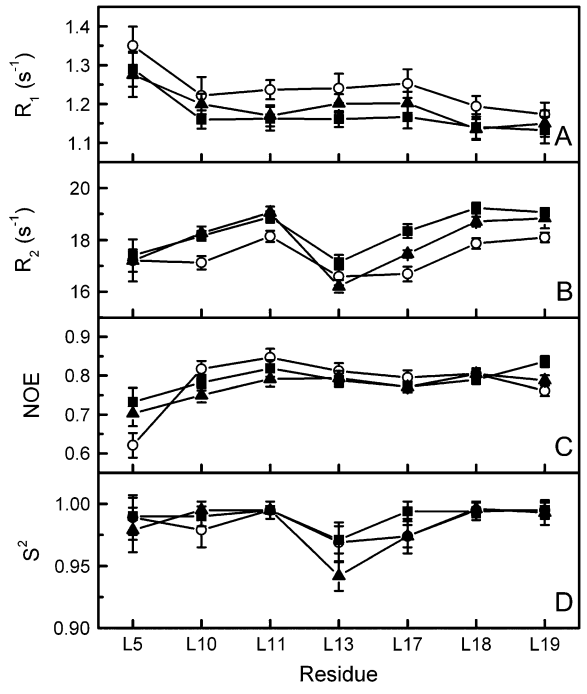

FIGURE 7 Relaxation rate constants R_1 (*A*) and R_2 (*B*), ^{15}N-[^{1}H] NOE values (*C*), and squared order parameters S^2 (*D*) for leucine amides of TM2e in DPC micelles in the absence of anesthetics (*squares*) and in the presence of 13 mM F3 (*circles*) and 9 mM isoflurane (*triangles*) at 30°C. The molar ratio of TM2e to DPC was 2:100. Errors were derived from the statistical dispersion and either from the uncertainties of the least-squares fit to the exponential decay function (for R_1 and R_2) or from the signal/noise ratios (for NOE). Error bars for S^2 (*D*) are standard deviations derived from 300 Monte Carlo simulations.

DISCUSSION

The STD experiments provided lines of evidence that both isoflurane and F3 directly interact with TM2e. However, the NOEs on anesthetic molecules from TM2e are small in comparison to those found from several globular proteins (39) but in a good agreement with what is observed in anesthetic interaction with transmembrane channel peptides (40). Smaller NOE on anesthetics in membrane proteins would be expected for at least two reasons. First, a large portion of anesthetics in membrane proteins interacted with lipids because of their good solubility in lipids (41,42). Second, it was shown that the on and off rates of isoflurane interacting with the nAChR were an order of magnitude higher than those with the globular protein BSA (9). The shorter life of anesthetic-protein complexes would lead to lower NOE values. The lock-and-key-type interaction, mostly found for ligand binding in enzymatic proteins, may not be a proper description for anesthetic interaction with channel proteins that are more relevant as anesthetic targets.

The STD experiments offered the answer to whether anesthetics directly interacted with TM2e. Chemical shift perturbation by anesthetics offered the clue for which part of TM2e anesthetics interacted with. One may not be able to rule out a possibility that anesthetic disturbed micelle structure and consequently altered TM2e conformation and changed the TM2e chemical shift. However, the confirmed direct anesthetic interaction with TM2e must have made dominant contributions to the TM2e chemical shift changes. Both isoflurane and F3 perturbed the chemical shift of L5 (locating it closer to the micelle periphery) to a similar extent, but isoflurane had a stronger effect than F3 on leucines closer to the TM2e center, such as L11. This may be related to the different geometric shapes of two anesthetics (Fig. 1): isoflurane is a linear molecule that can reach the TM2e residues more remote from its primary interaction site, whereas smaller and more compact F3 lacks this ability.

Among all leucine residues in TM2e, L5 showed a unique reaction to the addition of anesthetics. At a low concentration of anesthetics, L5 had the most significant chemical shift changes (Fig. 4). At higher concentrations of anesthetics (Fig. 2S), other residues became insensitive to additional anesthetics, but the L5 chemical shift changed steadily in response to increased anesthetic concentration. The uniqueness of L5 resulted from its special location in the TM2e structure and micelles. Our previous study (16) ascertained that L5 was located at the edge of the TM2e helix in the most labile water-micelle interface, whereas the other six leucines have more stable patterns of hydrogen bonding, as evidenced by their high degree of protection from amide exchange. It was suggested by our early studies (40,42,44,45) that preferred partition in the amphipathic region of a membrane

to its hydrophobic core was a characteristic of volatile general anesthetics related to their anesthetic activity. Therefore, the observed unique interaction between anesthetics and L5 confirms that the micelle-water interface is a place where anesthetics are distributed preferentially. Besides L5, L17, L18, L19, and I20 constitute a cluster of anesthetic-sensitive residues at the C-terminus of the TM2e helix, corresponding to the extracellular site of nAChR (Fig. 6). Similar locations of anesthetic sites near the C-terminus of TM2 have been pinpointed for the α and δ subunits of the muscle nAChR in photolabeling studies (12).

It is interesting to note that F3 had a minute effect on H_α but significantly affected the TM2e H_N (Fig. 5). The H_α chemical shifts are known to be sensitive to the secondary structures of proteins, and their differences from the random coil values are often used in protein secondary structure predictions (37,38). Insensitivity of H_α chemical shifts to anesthetics implied a well-preserved TM2e secondary structure in the presence of anesthetics. This is in accord with our previous finding on gramicidin, an ion channel peptide (44,45). Although anesthetics used for this study did not change the TM2e secondary structure, perturbation of the helix HBs seemed to be real. The up-field and down-field shifts of amide protons are often taken as evidence of lengthening or shortening of the corresponding HBs (46). Chemical shift oscillations for the amide protons in the middle region of TM2e occurred in a quasiperiodic fashion with the apparent periodicity of three or four residues (Fig. 5 *B*). The predicted pore-lining residues (T4, S8, L11, and V15) appear to be much less affected by anesthetics. Several residues adjacent to the pore-lining residues at either side seemed to be affected more. Such a pattern of hydrogen bond distortion across the peptide caused by nonsymmetric anesthetic interactions with the TM2e might also occur in the intact nAChR. The perturbation to the helical hydrogen bonding in the pore-lining domain, TM2, may generate impact to the channel properties, although it is hard to quantify such impact at present. Whether the subtle changes in the pore-lining domain will ultimately modify channel functions needs to be further investigated.

The correlation time τ_m for global tumbling of TM2e in DPC increased after addition of anesthetics to the sample, especially at a high anesthetic concentration. The diffusion of the TM2e-micelle complex was best described by an isotropic diffusion tensor both in the presence and absence of anesthetics. Without anesthetics, the τ_m value corresponded to the tumbling of the whole complex including the TM2e, a DPC micelle, and a hydration layer ($\sim$0.5 ns/kDa for isotropic tumbling according to the Stokes-Einstein model). The size of the complex became larger after addition of anesthetics. The τ_m rising from 11.7 to 12.3 ns in the absence and presence of isoflurane, respectively, could be ascribed primarily to the association of about five isoflurane molecules to the complex (estimated using the Stokes-Einstein model). Other conceivable mechanisms for the anesthetic-induced increase in τ_m could be through introduction of some degree of anisotropy in global tumbling or reduction of the peptide motion relative to the micelle (47,48). Because there was no strong indication of TM2e internal motion on the nanosecond timescale (16), it seemed unlikely that interdependence of internal and global motion contributed to the τ_m increase. The robustness of order parameters to anesthetics implied a minute anesthetic effect on the TM2e flexibility. The anesthetic molecules in the TM2e-micelle-anesthetic complex interacted not only with TM2e but also with DPC micelles. If associated anesthetics altered the micelle structure drastically so that the TM2e conformation and TM2e association with micelles were largely affected, it would be reflected in the TM2e backbone dynamics. The subtle change in τ_m and stable order parameters of the TM2e backbone do not support this possibility. The lack of evidence for significant changes in TM2e backbone dynamics could be caused by the timescale mismatching between TM2e backbone motion and NMR measurements. If the anesthetic-induced changes in TM2e internal dynamics occurred on a timescale different from pico- to nanoseconds, it would be undetectable by the conventional model-free analysis. Our attempts to search for TM2e internal motion on a micro- to millisecond timescale found no indication of such motion. Nevertheless, TM2e is only one of the four transmembrane domains in nAChR. The limited anesthetic effect on internal motion of the TM2e might be amplified once this pore-lining domain is integrated with other transmembrane domains. Indeed, we observed substantial anesthetic modulation on micro- to millisecond timescale motions of a four-helical bundle protein (T. Cui et al., article in review). Other previous studies also provided experimental evidence of anesthetic-induced changes in protein dynamics. Halothane and isoflurane decreased the mobility of the indole rings in BSA and stabilized BSA to thermal denaturation, as studied by fluorescence anisotropy and circular dichroism (49) as well as differential scanning microcalorimetry (50). Bromoform binding in the firefly luciferase crystal structure was shown to cause a neighboring histidine residue (H-310) to become less mobile (51). In addition, computational studies elucidated the potential importance of anesthetic modulation on protein dynamics (52). The global anesthetic effects on functional relevant motions of firefly luciferase have been revealed recently via Gaussian and anisotropic network analysis (53). Nevertheless, it is important to explore further the anesthetic effects on protein dynamics that ultimately affect protein functions. Research along this line on whole transmembrane domains of nAChR are in progress in our laboratory.

CONCLUSIONS

Taken together, we conclude that there is direct anesthetic interaction with the TM2e, especially at the helix N- and C-termini, which are situated at the micelle-water interface,

namely, in the vicinity of L5 and in the L17–L19 region. The ''saturatable'' nature of the chemical shifts of C-terminal L17–L19 region at elevated anesthetic concentrations marks the region with specific anesthetic interactions. In contrast, the anesthetic interaction with the N-terminal L5 seems less specific, as evidenced by the ''unsaturatable'' nature of L5 chemical shift at relatively high anesthetic concentrations. Although the presence of anesthetics did not significantly alter the TM2e secondary structure, the perturbation of the helix hydrogen bonding was implicated by a periodic change in the TM2e H_N chemical shifts. Preferable lengthening of HBs on one side and shortening on another side of the helix might induce a certain degree of helix bending. The anesthetic interaction had little impact on the TM2e backbone dynamics. Although the findings on a single TM2e domain are valuable, a study of anesthetic effects on the complete transmembrane domain and beyond is essential to gain more comprehensive insights into the anesthetic modulation of nAChR structure and dynamics and, ultimately, of nAChR functions (54).

SUPPLEMENTARY MATERIAL

To view all of the supplemental files associated with this article, visit www.biophysj.org.

The authors thank Dr. Zhanwu Liu for his assistance in sample preparation and initial NMR data acquisition. This work was supported in part by grants from the National Institutes of Health (R01GM56257 and R01GM66358 to P.T. and R37GM049202 to Y.X.).

REFERENCES

1. Karlin, A. 2002. Emerging structure of the nicotinic acetylcholine receptors. *Nat. Rev. Neurosci.* 3:102–114.
2. Hogg, R. C., M. Raggenbass, and D. Bertrand. 2003. Nicotinic acetylcholine receptors: from structure to brain function. *Rev. Physiol. Biochem. Pharmacol.* 147:1–46.
3. Sine, S. M., and A. G. Engel. 2006. Recent advances in Cys-loop receptor structure and function. *Nature.* 440:448–455.
4. Franks, N. P., and W. R. Lieb. 1994. Molecular and cellular mechanisms of general anaesthesia. *Nature.* 367:607–614.
5. Campagna, J. A., K. W. Miller, and S. A. Forman. 2003. Mechanisms of actions of inhaled anesthetics. *N. Engl. J. Med.* 348:2110–2124.
6. Forman, S. A., K. W. Miller, and G. Yellen. 1995. A discrete site for general anesthetics on a postsynaptic receptor. *Mol. Pharmacol.* 48: 574–581.
7. Yamakura, T., C. Borghese, and R. A. Harris. 2000. A transmembrane site determines sensitivity of neuronal nicotinic acetylcholine receptors to general anesthetics. *J. Biol. Chem.* 275:40879–40886.
8. Wenningmann, I., M. Barann, A. M. Vidal, and J. P. Dilger. 2001. The effects of isoflurane on acetylcholine receptor channels: 3. Effects of conservative polar-to-nonpolar mutations within the channel pore. *Mol. Pharmacol.* 60:584–594.
9. Xu, Y., T. Seto, P. Tang, and L. Firestone. 2000. NMR study of volatile anesthetic binding to nicotinic acetylcholine receptors. *Biophys. J.* 78: 746–751.
10. Eckenhoff, R. G. 1996. An inhalational anesthetic binding domain in the nicotinic acetylcholine receptor. *Proc. Natl. Acad. Sci. USA.* 93:2807–2810.
11. Chiara, D. C., L. J. Dangott, R. G. Eckenhoff, and J. B. Cohen. 2003. Identification of nicotinic acetylcholine receptor amino acids photolabeled by the volatile anesthetic halothane. *Biochemistry.* 42:13457–13467.
12. Ziebell, M. R., S. Nirthanan, S. S. Husain, K. W. Miller, and J. B. Cohen. 2004. Identification of binding sites in the nicotinic acetylcholine receptor for [^{3}H]azietomidate, a photoactivatable general anesthetic. *J. Biol. Chem.* 279:17640–17649.
13. Miyazawa, A., Y. Fujiyoshi, and N. Unwin. 2003. Structure and gating mechanism of the acetylcholine receptor pore. *Nature.* 423:949–955.
14. Unwin, N. 2005. Refined structure of the nicotinic acetylcholine receptor at 4A resolution. *J. Mol. Biol.* 346:967–989.
15. Yeagle, P. L., and A. D. Albert. 2007. G-protein coupled receptor structure. *Biochim. Biophys. Acta.* 1768:808–824.
16. Yushmanov, V. E., Y. Xu, and P. Tang. 2003. NMR structure and dynamics of the second transmembrane domain of the acetylcholine receptor β_2 subunit. *Biochemistry.* 42:13058–13065.
17. Bondarenko, V., Y. Xu, and P. Tang. 2007. Structure of the first transmembrane domain of the neuronal acetylcholine receptor {beta}2 subunit. *Biophys. J.* 92:1616–1622.
18. Flood, P., J. Ramirez-Latorre, and L. Role. 1997. Alpha 4 beta 2 neuronal nicotinic acetylcholine receptors in the central nervous system are inhibited by isoflurane and propofol, but alpha 7-type nicotinic acetylcholine receptors are unaffected. *Anesthesiology.* 86:859–865.
19. Violet, J. M., D. L. Downie, R. C. Nakisa, W. R. Lieb, and N. P. Franks. 1997. Differential sensitivities of mammalian neuronal and muscle nicotinic acetylcholine receptors to general anesthetics. *Anesthesiology.* 86:866–874.
20. Piotto, M., V. Saudek, and V. Sklenar. 1992. Gradient-tailored excitation for single-quantum NMR spectroscopy of aqueous solutions. *J. Biomol. NMR.* 2:661–665.
21. Marion, D., and K. Wuthrich. 1983. Application of phase sensitive two-dimensional correlated spectroscopy (COSY) for measurements of ^{1}H–^{1}H spin-spin coupling constants in proteins. *Biochem. Biophys. Res. Commun.* 113:967–974.
22. Mayer, M., and B. Meyer. 1999. Characterization of ligand binding by saturation transfer difference NMR spectroscopy. *Angew. Chem. Int. Ed.* 38:1784–1788.
23. Hwang, T. L., and A. J. Shaka. 1995. Water suppression that works—excitation sculpting using arbitrary wave-forms and pulsed-field gradients. *J. Magn. Reson. A.* 112:275–279.
24. Farrow, N. A., R. Muhandiram, A. U. Singer, S. M. Pascal, C. M. Kay, G. Gish, S. E. Shoelson, T. Pawson, J. D. Forman-Kay, and L. E. Kay. 1994. Backbone dynamics of a free and phosphopeptide-complexed Src homology 2 domain studied by ^{15}N NMR relaxation. *Biochemistry.* 33:5984–6003.
25. Schleucher, J., M. Schwendinger, M. Sattler, P. Schmidt, O. Schedletzky, S. J. Glaser, O. W. Sorensen, and C. Griesinger. 1994. A general enhancement scheme in heteronuclear multidimensional NMR employing pulsed field gradients. *J. Biomol. NMR.* 4:301–306.
26. Kay, L., P. Keifer, and T. Saarinen. 1992. Pure absorption gradient enhanced heteronuclear single quantum correlation spectroscopy with improved sensitivity. *J. Am. Chem. Soc.* 114:10663–10665.
27. Wishart, D. S., and D. A. Case. 2001. Use of chemical shifts in macromolecular structure determination. *Methods Enzymol.* 338:3–34.
28. Delaglio, F., S. Grzesiek, G. W. Vuister, G. Zhu, J. Pfeifer, and A. Bax. 1995. NMRPipe: a multidimensional spectral processing system based on UNIX pipes. *J. Biomol. NMR.* 6:277–293.
29. Goddard, T. D., and D. G. Kneller. 2001. SPARKY 3. University of California, San Francisco.
30. Kay, L. E., D. A. Torchia, and A. Bax. 1989. Backbone dynamics of proteins as studied by ^{15}N inverse detected heteronuclear NMR spectroscopy: application to staphylococcal nuclease. *Biochemistry.* 28: 8972–8979.
31. Lipari, G., and A. Szabo. 1982. Model-free approach to the interpretation of nuclear magnetic resonance relaxation in macromolecules. 1. Theory and range of validity. *J. Am. Chem. Soc.* 104:4546–4559.

32. Lipari, G., and A. Szabo. 1982. Model-free approach to the interpretation of nuclear magnetic resonance relaxation in macromolecules. 2. Analysis of experimental results. *J. Am. Chem. Soc.* 104:4559–4570.

33. Palmer III, A. G., M. Rance, and P. E. Wright. 1991. Intramolecular motions of a zinc finger DNA-binding domain from Xfin characterized by proton-detected natural abundance carbon-13 heteronuclear NMR spectroscopy. *J. Am. Chem. Soc.* 113:4371–4380.

34. Mandel, A. M., M. Akke, and A. G. Palmer III. 1995. Backbone dynamics of *Escherichia coli* ribonuclease HI: correlations with structure and function in an active enzyme. *J. Mol. Biol.* 246:144–163.

35. Dosset, P., J.-C. Hus, M. Blackledge, and D. Marion. 2000. Efficient analysis of macromolecular rotational diffusion from heteronuclear relaxation data. *J. Biomol. NMR.* 16:23–28.

36. Qin, J., O. Vinogradova, and A. M. Gronenborn. 2001. Protein-protein interactions probed by nuclear magnetic resonance spectroscopy. *Methods Enzymol.* 339:377–389.

37. Wishart, D. S., B. D. Sykes, and F. M. Richards. 1992. The chemical-shift index—a fast and simple method for the assignment of protein secondary structure through NMR- spectroscopy. *Biochemistry.* 31:1647–1651.

38. Wishart, D. S., and B. D. Sykes. 1994. Chemical shifts as a tool for structure determination. *Methods Enzymol.* 239:363–392.

39. Streiff, J. H., N. O. Juranic, S. I. Macura, D. O. Warner, K. A. Jones, and W. J. Perkins. 2004. Saturation transfer difference nuclear magnetic resonance spectroscopy as a method for screening proteins for anesthetic binding. *Mol. Pharmacol.* 66:929–935.

40. Tang, P., J. Hu, S. Liachenko, and Y. Xu. 1999. Distinctly different interactions of anesthetic and nonimmobilizer with transmembrane channel peptides. *Biophys. J.* 77:739–746.

41. Firestone, L. L., J. C. Miller, and K. W. Miller. 1986. Tables of physical and pharmacological properties of anesthetics. In Molecular and cellular mechanisms of anesthetics. S. H. Roth, and K. W. Miller, editors. Plenum, New York. 455–470.

42. Tang, P., B. Yan, and Y. Xu. 1997. Different distribution of fluorinated anesthetics and nonanesthetics in model membrane: a 19F NMR study. *Biophys. J.* 72:1676–1682.

43. Reference deleted in proof.

44. Tang, P., V. Simplaceanu, and Y. Xu. 1999. Structural consequences of anesthetic and nonimmobilizer interaction with gramicidin A channels. *Biophys. J.* 76:2346–2350.

45. Tang, P., R. G. Eckenhoff, and Y. Xu. 2000. General anesthetic binding to gramicidin A: the structural requirements. *Biophys. J.* 78: 1804–1809.

46. Zhou, N. E., B. Y. Zhu, B. D. Sykes, and R. S. Hodges. 1992. Relationship between amide proton chemical-shifts and hydrogen-bonding in amphipathic alpha-helical peptides. *J. Am. Chem. Soc.* 114:4320–4326.

47. Krueger-Koplin, R. D., P. L. Sorgen, S. T. Krueger-Koplin, I. O. Rivera-Torres, S. M. Cahill, D. B. Hicks, L. Grinius, T. A. Krulwich, and M. E. Girvin. 2004. An evaluation of detergents for NMR structural studies of membrane proteins. *J. Biomol. NMR.* 28:43–57.

48. Chill, J. H., J. M. Louis, J. L. Baber, and A. Bax. 2006. Measurement of ^{15}N relaxation in the detergent-solubilized tetrameric KcsA potassium channel. *J. Biomol. NMR.* 36:123–136.

49. Johansson, J. S., H. Zou, and J. W. Tanner. 1999. Bound volatile general anesthetics alter both local protein dynamics and global protein stability. *Anesthesiology.* 90:235–245.

50. Tanner, J. W., P. A. Liebman, and R. G. Eckenhoff. 1998. Volatile anesthetics alter protein stability. *Toxicol. Lett.* 100–101:387–391.

51. Franks, N. P., A. Jenkins, E. Conti, W. R. Lieb, and P. Brick. 1998. Structural basis for the inhibition of firefly luciferase by a general anesthetic. *Biophys. J.* 75:2205–2211.

52. Tang, P., and Y. Xu. 2002. Large-scale molecular dynamics simulations of general anesthetic effects on the ion channel in the fully hydrated membrane: the implication of molecular mechanisms of general anesthesia. *Proc. Natl. Acad. Sci. USA.* 99:16035–16040.

53. Szarecka, A., Y. Xu, and P. Tang. 2007. Dynamics of firefly luciferase inhibition by general anesthetics: gaussian and anisotropic network analyses. *Biophys. J.* 93:1895–1905.

54. Szarecka, A., Y. Xu, and P. Tang. 2007. Dynamics of heteropentameric nicotinic acetylcholine receptor: implications of the gating mechanism. *Proteins.* 68:948–960.